Identification by suppression subtractive hybridization and expression analysis of *Medicago truncatula* putative defence genes in response to *Orobanche crenata* parasitization

José Vicente Die[1]*, Miguel A. Dita[2], Franziska Krajinski[3], Clara I. González-Verdejo[1], Diego Rubiales[2], M Teresa Moreno[1], Belén Román[1]

[1]IFAPA-CICE, Centro ‘‘Alameda del Obispo’’ S/N Apdo. 4084, 14080 Córdoba, Spain

[2]CSIC, Institute for Sustainable Agriculture, Apdo. 4084, 14080 Córdoba, Spain

[3]Lehrgebiet Molekulargenetik, Universität Hannover, 30419 Hannover, Germany

*Corresponding author(s). E-mail(s): jose.die@juntadeandalucia.es;

Abstract

Crenate broomrape (Orobanche crenata) is the major constraint for pea and faba bean production in the Mediterranean region. In this study, a systematic sequencing of expressed sequence tags (ESTs) was chosen to obtain a first global picture of the assembly of genes involved in defence response. A cDNA-library was established by suppression subtractive hybridization in the model legume Medicago truncatula infected by O. crenata in order to identify a large number of host plant ESTs. Eighty-one presumably up-regulated genes were identified and classified in functional categories. EST-annotations showed homologies to a number of well-characterized genes. Most of the proteins encoded by these genes, are already known in defence in M. truncatula, such as genes related to the JA pathway or involved in cell wall modifications. A notable number of the ESTs, however, were derived from novel genes not matching entries of the large-scale M. truncatula sequences collections. Expression analyses by quantitative RT-PCR of 20 genes corresponding to different functional categories showed high expression levels, supporting their involvement in the defence response.

Keywords: Medicago truncatula; Orobanche crenata; Real-time RT-PCR; SSH

1 Introduction

Crenate broomrape (Orobanche crenata Forsk.) is a holoparasitic weed that seriously attacks legume crops, such as faba bean, lentils, pea, chickpea and vetch. This parasitic plant is considered the major constraint for legume crops in Mediterranean countries [1,2]. The Orobanche seeds germinate in response to a chemical signal exuded from host roots. Subsequently, the radicle of the parasite develops into a haustorium, a specialized structure that penetrates the host root and forms a connection between the host vascular tissue and the parasite. Once the connection is established, the parasite develops into a tubercle, a bulbous structure from which a shoot emerges from the soil to flower and produce seeds. Control methods have been focused mainly on cultural practices and herbicides application. However, only limited success has been achieved so far [1]. The best long-term strategy for limiting damage caused by O. crenata is the development of resistant crops, but only incomplete levels of resistance have been achieved in grain legumes by traditional plant breeding [2,3]. There is a strong consensus that detailed knowledge of the molecular mechanisms underlying the host–parasite interaction is necessary to improve breeding programmes. Understanding the mechanisms that regulate the expression of parasite-related genes is a fundamental issue and will be necessary for the genetic improvement of legumes [4]. However, only very little is known about the changes of gene expression in parasitized plants and the molecular basis of resistance. First studies in this sense based on target-gene approaches using plant models (e.g. Nicotiana tabacum), offered significant advances about transcriptional changes occurring in parasitized plants [5,6]. Further gene-target expression studies showed the involvement of several Arabidopsis thaliana genes in the response to O. ramosa infection [7]. Induction of genes related to ethylene and jasmonate pathways were detected, even before parasite attachment on the host roots. The same authors using a subtractive suppression hybridization (SSH) approach reported the identification of 13 differentially expressed genes in this interaction [8]. These early studies revealed the complexity of defence patterns against parasitic plants and the necessity to obtain more comprehensive knowledge of the molecular events involved in host–parasitic plant response.

In recent years, high-through expression profiling technologies have transformed significantly molecular genetics approaches in legumes. The emergence of ‘‘omic’’ technologies and the establishment of model legume plant Medicago truncatula are promising strategies for understanding the molecular genetic basis of stress resistance, which is an important bottleneck for molecular breeding [9]. The fact that M. truncatula can be infected by O. crenata [10] opened the possibility to use this model plant to gain knowledge of the molecular response to this parasite in legumes.

A genome sequencing project for M. truncatula is underway [11]. The Institute for Genomic Research (TIGR) M. truncatula Gene Index (MtGI) have generated over 225 000 (release 8.0, January 2005) expressed sequence tags (ESTs) from more than 60 cDNA libraries representing genes expressed in different M. truncatula tissues, developmental stages and growth conditions. Based on a subset of the M. truncatula sequences available in EST databases, a 16 086 probe oligo microarrays (Mt16kOLI1) was constructed, being to date the most comprehensive array representation of M. truncatula genes [12,13]. Using this microarray we have obtained the first insight of gene expression of M. truncatula in response to O. crenata (Dita et al., unpublished results). Nevertheless, most genes present on this microarray are from symbiotic associations but not from cDNA libraries enriched from parasitic–plant interactions. Additionally, due to the tight shown regulation of significant plant genes with respect to the timing and localization of expression, they tend to be underrepresented in the non-enriched cDNA libraries, and hence, are difficult to detect on the basis of cDNA-based microarray hybridizations. Thus, other strategies are needed in order to identify new and/or specific differentially expressed genes in the M. truncatula–O. crenata interaction.

The aim of the present study was to carry out a suppression subtractive hybridisation (SSH) cDNA-library enriched for clones corresponding to genes regulated during infection by O. crenata in order to analyze the transcriptional profile of M. truncatula during this interaction.

Cold tolerance in plants is a complex trait that involves a huge number of genes and metabolites [11]. Analyses of the transcriptomes and metabolomes of *Poa crymophila* [12] and *Nicotiana tabacum* [13] have been conducted to determine the key metabolites, regulatory mechanisms, and candidate genes involved in the response of these plants to cold stress. Several studies have demonstrated that multiple genes regulate the responses of various organisms to low temperatures. The molecular mechanisms that regulate plant cold stress responses have preliminarily been elucidated by analyzing differentially expressed genes (especially transcription factors) between cold-tolerant and cold-sensitive lines [14-16]. For example transcription factors such as bHLH, NAC, C2H2, MYB, WRKY and AP2/ERF were identified in asparagus bean [17] and rice [18] exposed to low-temperature stress. Moreover, two major families of transcription factors, AP2-EREBP and bHLH, display altered expression in *Magnolia*

wufengensis during cold stress [19]. Moreover, metabolomic analysis showed that the content of flavonols such as quercetin and dihydromyricetin increased significantly in *Brassica napus* exposed to cold stress [20]. In addition, a variety of metabolites, particularly flavonoids, have been found to play important roles in the response of plants to cold stress [21].

The CBF/DREB1 gene family has been demonstrated to respond to a variety of environmental stressors in lettuce, including cold, heat and salinity [22]. LsCBF5, LsCBF7, LsCBF11, LsCBF12 and LsCBF14 are upregulated in response to cold and heat stress, which implies that these genes regulate the response to abiotic stress and enable lettuce to adapt to a broader range of environmental conditions. Additionally, we previously reported that various metabolites and transcription factors are involved in the response of lettuce to heat [23]. While these previous studies demonstrate that numerous metabolites play important roles in the cold stress response of lettuce, further research is needed to explore the precise functions of these metabolites and there is a lack of research on the molecular mechanisms involved in the responses of lettuce under cold stress.

Thus, in this study, two cold-tolerant and two cold-sensitive lettuce varieties were selected from 275 cultivars for further transcriptomic and metabolomic analysis. Bioinformatic analyses were performed to identify the major metabolites, regulatory pathways, and candidate genes involved in the response of the cold-tolerant and cold-sensitive cultivars to cold stress. We demonstrate that the flavonoid metabolic pathway is involved in the response of lettuce to cold stress. Overall, these mechanistic insights could be leveraged to develop new biological regulators to protect lettuce plants against cold stresses or to breed new lettuce varieties with improved cold tolerance.

2 Material and Methods

2.1 Plant material, growth conditions and inoculation

The M. truncatula genotype SA4087 (incomplete late resistance) was selected based on previous experiments [10]. Seeds of M. truncatula were surface-sterilized (NaClO 0.05%) and pre-germinated in filter paper. Seedlings with roots between 5 and 7 cm were placed in squared Petri dishes (12 cm 12 cm) containing a sheet of glass-fibre filter paper (GFFP; Whatman International, Kent, UK), and perlite as substrate. When seedlings presented at least one true leaf, they were inoculated with O. crenata seeds (Co´rdoba population) at a density of 50 seeds/cm2 . O. crenata seeds had previously been surface-sterilized [14] and stored in the dark at 20 1C during 8 days to promote conditioning of broomrape seeds necessary for germination. The synthetic germination stimulant GR24 was applied by adding 3 mL of a 0.034 mM solution [15]. Dishes were sealed with parafilm, covered with aluminium foil to prevent roots and broomrape seeds from the light, placed vertically the germinating host plant upwards in trays with Hoagland nutrient solution and kept in the growing chamber at 20 1C with 14 h light [16]. Three serial experiments using 30 plants per experiment were performed. Fifteen of these plants were infected and the other 15 used as non-infected controls.

2.2 Sample collection and RNA extraction

Roots were harvested at 15 (first contacts of O. crenata radicles with host roots), 21 (initial stage of tubercle formation) and 35 days (prior to necrosis of well-developed parasite tubercle) post inoculation (Fig. 1). In order to avoid contamination with parasite tissues, host roots were abundantly washed with distilled water and blot dried with filter paper. Parasite tubercles collected at 21 and 35 days post inoculation (dpi) were carefully removed by cutting the attachment organ without wounding the host roots. Non-infected roots used as control were also abundantly washed with distilled water and blot dried with filter paper. Collected samples were immediately frozen in liquid nitrogen and stored at 80 1C. Total RNA samples isolated from roots were prepared using TRIZOL reagent (Invitrogen, Carlsbad, CA, USA) according to manufacture's protocols from different pools of five roots in both, infected and control roots, in order to minimize variation in gene expression among individual plants. The resulting RNA preparations were stored at 80 1C until use. The integrity of total RNA was checked on agarose gels and its quantity as well as purity was determined spectrophotometrically.

2.3 Screening of DEGs involved in cold tolerance SSH and cDNA-library construction

SSH [17] was used to generate a cDNA-library enriched for sequences induced in M. truncatula roots in response to O. crenata infection. In order to obtain a SSH-library representative of genes expressed differentially along the main stages of parasitization process, before cDNA synthesis, RNA samples collected in the different time points were equally pooled (Fig. 2). Total RNA (1.5 mg) was reverse-transcribed and amplified using the SMART PCR cDNA Synthesis kit (Clontech, Palo Alto, CA, USA) according to the user manual. Total RNA derived from non-infected roots and O. crenata were pooled 20:1 and used as driver population. The SMART-cDNAs were size-selected through a NucleoSpin Extract kit (Macherey-Nagel, Du¨ren, Germany). The double strand cDNA fractions were digested with RsaI to obtain shorter, blunt-ended molecules, then purified with a phenol–chloroform–isoamyl alcohol (25:24:1). The purified RsaI-digested cDNAs were precipitated by 4 M ammonium acetate and absolute ethanol. The cDNA pellet was washed in 80% ethanol and dissolved in 6.7 of H2O to obtain cDNAs at a concentration of 300 ng/mL. SSH was performed using the PCR-select cDNA subtraction kit (Clontech, Palo Alto, USA), following the manufacture's instructions. The SSH-library enriched for differentially expressed cDNAs was constructed by insertion of the subtracted cDNAs into pGEM-Teasy vector (Promega, Madison, USA), and transformed into supercompetent Escherichia coli XL1-Blue MRF' cells (Stratagene, La Jolla, CA). Three hundred colonies of transformed bacteria harboring the cDNA clones were stored in glycerol at -80ºC.

2.4. cDNA sequencing and data analyses

Clones of the SSH library were manually picked and sequenced (IIT-Biotech, Bielefeld, Germany). To cluster and annotate the sequences obtained, the Sequence Analysis and Management System (SAMS v.1.4, Cebitec Bielefeld University, Germany) software package was used. This software processes sequence data as follows: initially, a normalization step using PHRED [18] is performed with the raw EST trace files. Afterward, low quality regions are removed according to the PHRED13 quality definition [19]. Finally the sequences are trimmed to eliminate vector, SMART-cDNA-primer and SSH-adaptor sequences. Vector clipping lead to EST reads in FASTA file format. Clustering of the EST reads also was performed by the SAMS package according to an implementation of the TIGR clustering algorithm [20] using a minimum length of 40 bp, sequence identity of at least 95%, and enlarged and assembled with CAP3 contig assembly program of cluster EST members [21]. The sequence data obtained correspond to tentative consensus sequences (TCs) and single (unclustered) EST reads, or singletons. Further nucleotide alignments were performed and some singletons were reclassified as members of established TCs. Comparisons to the TIGR MtGI

were done in order to identify identical TCs sequences. Annotations were manually checked by means of BLASTx searches for homologous genes in other organisms [22].

2.5 Data validation by quantitative real-time RT-PCR

Quantitative real-time reverse transcriptase-polymerase chain reaction (RT-PCR) was carried out using the QuantiTec SYBR Green RT-PCR Master Mix One-Step (Quiagen, Hilden, Germany). Three independent experiments were used as biological repetitions to extract total RNA, with one repetition corresponding to the RNA used for cDNA-library construction. The two new sets of infected and non-infected control plants were grown and collected at the same time points after inoculation and total RNA was isolated from different pools of five roots using Trizol reagent as described above. Dnase I-treated (Turbo DNA-free, Ambion, USA) RNA preparations were checked for the absence of DNA contamination by a control PCR using Tefa primers. Total RNA (50 ng) was used in a total volume of 25 ml. Reactions were run on the Mx3000P real-time PCR system (Stratagene, La Jolla, CA, USA) and quantification was performed with the Mx3000P analysis software version 3.00. The following run protocol was used: reverse transcription (50 1C for 30 min), polymerase activation (95 1C for 10 min), amplification and quantification cycles repeated 44 times (95 1C for 30 s, 55 1C for 1 min, 72 1C for 30 s, with a single fluorescence measurement), and dissociation curve (55–95 1C with one fluorescence read every 0.5 1C). The gene-specific primers used for RT-PCR (Table 1) were designed with a calculated Tm of 5370.1 1C, amplification products not larger than 360 bp, and the primer sequences were unique in the TIGR MtGI. A relative expression ratio was calculated as the ratio of normalized gene expression of the gene of interest against a constitutively expressed M. truncatula gene that encodes an elongation factor 1-alpha (MtTefa TC106485, TIGR MtGI) as described by Hohnjec et al. [23]. We tested each genes three technical replicates and performed a Student's t test to calculate the significance of relative expression values between the expression levels in infected roots compared with the corresponding control roots and the average ratio of these values was used to determine the fold change in transcript level in infected samples compared with controls.

3 Results

3.1 Data validation by quantitative real-time RT-PCR

A cDNA library was generated by SSH to obtain a large number of ESTs, representing genes up-regulated in M. truncatula roots parasitized by O. crenata (Table 2). PCR fragments were cloned and 288 ESTs were obtained with an average valid read-length of 546 bp. SSH–cDNA sequences with a length of more than 50 bp were designated as MtOROCRE (M. truncatula–O. crenata) and submitted to the GenBank database and can be accessed under accession numbers EH058234–EHO58497.

3.2. ESTs clustering and annotation

ESTs clustering according to the TIGR protocol revealed 33 tentative consensus (TC) sequences and 89 singletons with an average of 6.03 ESTs per TC. P450 trans-cinnamate 4-monooxygenase protein (TC106704), assembled from 26 SSH-ESTs was the most redundant sequence in the cDNA population (Table 3). In order to obtain a higher quality of annotation, we reannotated EST clusters manually based on comparisons to the current releases of the UniProt (http://www.pir.uniprot.org) and InterPro (http://www.ebi.ac.uk/interpro) databases. Subsequently, the proteins encoded by Orobanche-induced M. truncatula genes were grouped into functional categories according to Journet et al. [24]. It was possible to assign putative functions to about 65% of the ESTs in the library. More than 90 sequences encoded proteins with insufficient similarity to proteins of known function to assign a function with confidence (unknown function) and surprisingly 35 out of these sequences did not match any EST deposited in the MtGI (v. 8.0). Among these 35 ESTs, 32 did not show any significant similarity (using an e-value cut off of 1e10) after BLASTx search on the GenBank database. Further nucleotide alignments reclassified some singletons as members of both, established and new TCs. Thus, the initial 288 fragments sequenced, identified a total of 81 different genes grouped into 37 TCs and 44 singletons with a sequence length more than 100 bp. On average, 69.66% of the sequences in the library were redundant. Genes with known function were sorted into 12 primary functional categories [24]. The distribution of the functional classification is represented in Fig. 3. The largest set of induced genes (11.1%) was assigned to the secondary metabolism category, while genes involved in cell division cycle constituted the smallest group, comprising less than 1.5% of the genes. Genes encoding proteins involved in primary metabolism (9.9%) and signal transduction (7.1%) and RNA metabolism (7.1%) formed the second and third largest group, respectively. Genes involved in defence and cell rescue resulted in 3.7% of the library. Sequence annotations of differentially expressed SSH–cDNAs aligned to TCs are shown in Table 3.

3.3 Relative quantification of gene expression by real-time reverse transcriptase-polymerase chain reaction

We performed quantitative real-time RT-PCR to verify the experimental expression pattern of 20 putative Orobanche-induced M. truncatula genes corresponding to a range of functional categories, with the most prominent classes being secondary and hormone metabolism (five genes) as well as cell wall (four genes). All primers were used to amplify genomic DNA of M. truncatula and O. crenata. Amplification PCR products were obtained for all genes in M. truncatula but no amplification products were visualized with O. crenata DNA template (data not shown), proving that all genes selected originated from M. truncatula and not from the parasite. After RT-PCR, the specificity of the PCR products obtained was analyzed by performing a heat dissociation protocol following the final cycle of the PCR and for all reactions which presented single amplification products (Table 4), gene induction levels calculated on the basis of the three biological repetitions and the technical replications were estimated. Transcripts of MtEf-1a gene, selected as constitutive expressed control for normalization showed a constant expression (the average CT value was 19.6070.67 among the RNA samples/plates tested) and set 1. None of the analyzed genes reached the level of MtEf-1a. The induction of a receptor-like protein kinase (TC94311) reached a relative expression level of 0.213 in infected roots, the highest comparative expression level measured in this study. Thrirteen out of the 20 genes tested were found induced in the analyzed samples. Eleven of these genes were verified to be at least 1.7-fold induced in infected M. truncatula roots and nine showed more than 2-fold difference in their RNA accumulation level with a P value p0.05. The most strongly Orobanche-induced gene, a dehydrin-like protein (TC100921) which shares 90.68% identity to a dehydrin reported in M. sativa during cold acclimation [25], was more than 240-fold difference of expression level in infected roots compared with the corresponding controls.

4 Discussion

The plant response to parasitic plants is a highly complex event determined by a number of different factors involving the coordinated regulation of thousands of genes of different cellular process acting at different levels during the infection. Orobanche has been shown to have a series of developmental steps, each one crucial to ensure and develop the infection [26]. Different sources of resistance to Orobanche spp. acting at these steps have been described which include pre-penetration [27–29], postpenetration [16,30,31] and postestablishment mechanisms [32]. The main developmental stages have been suggested as potentially key to neutralize the parasite [26,33]. But to date, information about the molecular events or the use of transcriptomic tools reflecting the overall response to parasitism is scarce. In this study, using a non-targeted SSH approach, a cDNA-library enriched for O. crenata-induced genes in M. truncatula was established representing the host response to the early steps of Orobanche infection from the broomrape radicles contacting the host roots to welldeveloped tubercles. In the late resistance M. truncatula accession SA4087, tubercles are developed but most of them become necrotic later reducing significantly the emergence of flowering shoots. Its ability to allow different developmental steps of the parasitization process, makes it a suitable genotype for Medicago–Orobanche interaction studies [10,34, Dita et al., unpublished results]. Some genes presented in this study have been previously described in arbuscular mycorrhizal symbiose or Orobanche parasitization identified by transcription profiling [12,35] or substractive hybridization [8,36,37]. Sequence analysis of the 81 ESTs indicated that the library was enriched in defence-related genes, representing more than 3.7% of the total ESTs compared with less than 2.5% in non-pathogenesis-related M. truncatula libraries [38]. Such a ratio probably underestimated the real number of genes potentially involved in plant defence or resistance in the library, notably because according to the classification followed, the functional categories ‘‘cellwall’’, ‘‘signalling’’ and ‘‘secondary pathway’’ may also be involved in plant defence and were categorized separately.

To gain information on the genetic program of M. truncatula during O. crenata parasitization, only a range of genes with putative or unknown functions, but matching sequences collections, have been further studied for their RNA accumulation pattern in infected and control roots. Transcriptional changes observed by subtraction and hybridization method were confirmed by quantitative real-time RT-PCR. Thirteen out of the 20 analyzed M. truncatula genes showed higher RNA accumulation in infected roots. Nearly all the 13 Orobancheinduced genes showed detectable expression in control roots RNA. This indicates that the corresponding genes are transcribed at basal level in non-infected roots but are significantly up-regulated after Orobanche infection. The screening of 20 SSH genes resulted in 55% up-regulated genes being at least 1.7-fold induced in infected M. truncatula roots. This is comparable with the ratio in other SSH libraries where levels of differentially expressed genes have been reported to range from less than 10% and up to 95% and to depend mainly on the biological material [39]. This validates the choice of the SSH strategy and the real-time RT-PCR experiments to support transcriptional changes observed in order to identify Orobanche-induced M. truncatula genes.

The most redundant sequence in the library, a P450 trans-cinnamate 4-monooxygenase gene belongs to a P450- type cytochrome which mediates a wide range of oxidative reactions involved in the biosynthesis of plant secondary metabolites including those associated to pathogen defence as phenylpropanoids and phytoalexins [40,41] and is related to the jasmonic acid pathway [42,43]. The induction of defence-related genes is part of the response triggered in legume host plants during pathogenic interactions [38]. The grouping into functional categories revealed that several cDNAs belong to defence genes. Among the genes showing high induction in M. truncatula roots was a hsr203J homolog (TC107779). This EST shares 80.99% identity to a hypersensitivity-related protein hsr203J with abundant transcripts induced by fungal elicitor in Pisum sativum [44]. Activation of hsr203J was first described in N. tabacum showing RNA accumulation preferentially during the incompatible interaction of tobacco with the pathogenic bacterium Pseudomonas solanacearum [45]. Functional characterization of the gene product has shown that hsr203J encodes a serine hydrolase that displays esterase activity [46]. It is unclear whether this gene plays an active role in cell death response or weather it acts as a regulator in the reaction and its function in the Orobanche interaction remains to be elucidated. Although hypersensitive-like responses (HR) have been evidenced in the plant–parasitic plant interaction cowpea–Striga [47], the existence of HR in Orobanche and its legumes host has been to date ruled out [16,48].

Cell wall strengthening and reinforcement as a physical barrier to prevent the parasite penetration into the host has been also reported as a principal mechanism of resistance in legumes [16]. In this sense, an up-regulated gene encoding a cinnamoyl CoA reductase (CCR) identified by SSH was assessed. CCR is the first enzyme specific to the biosynthetic pathway leading to lignin monomers [49–51] and their involvement in cell wall reinforcement and differentially expression in response to infection has been shown in A. thaliana during the interaction with the pathogenic bacteria Xanthomonas campestris [52]. Although the importance of cell wall modifications is

reflected in the number of ESTs (more than 6% of the library grouped into this functional category), it seems not to be a clear response in Medicago SA4087–O. crenata interaction based on the transcriptional changes detected by SSH. The major relevance of other categories suggests the coexistence of some other types of defence mechanisms which are still unclear.

On the other hand, it becomes evident that transcript accumulation in infected roots responding directly to Orobanche and abiotic signalling pathways as general feature of defence-related response may share multiple nodes and their outputs may have significant functional overlap. In this way, a range of cDNA clones associated with abiotic stimuli response were identified in the library. Induction of a gene encoding a ripening-related protein (TC106505) was verified by real-time RT-PCR. Most of the 15 ESTs reported in TC106505 in MtGI, derived from cDNA libraries constructed from M. truncatula during several pathogenic interactions. Searches against the InterPro database [53] revealed a domain similar to InterPro entry IPR000916 for Bet v I allergen which belongs to a group of protein family, including intracellular pathogenesis-related proteins of the PR-10 group [54], heavily inducible under senescence and stress conditions, as well as by plant signal molecules such as ABA, SA, JA or ethylene [55]. The most strongly Orobanche-induced gene in this study was a dehydrin-like protein (TC100921). In MtGi database, 31 ESTs are aligned to the TC100921 which are originated from various tissues and physiological conditions but none of them derived from a pathogenic interaction library. Nearly half of the number of entries of this TC sequence are deriving from M. truncatula plantlets under drought stress. This seems to reveal that common mechanisms could be shared by the response to drought and Orobanche. Although water losses via the parasite can be low in some parasitic species [56], there is evidence to greater loss of water from Orobanche infected plants when compared with non-infected controls [57]. The strong induction of a gene encoding a dehydrin-like protein in response to Orobanche might comprise part of the alterations in host metabolism necessary to overcome the water deficiency caused by the parasite. The induction of a set of defence-related genes not only to biotic but also to abiotic stimuli points to a connection between these two types of stresses at the molecular level indicating a functional overlap between biotic and abiotic signalling pathways in response to O. crenata.

Another observation resulting from the EST analysis is the high number of TCs sequences encoding protein with unknown functions. It would be interesting to confirm these modifications of transcript levels with more experimental evidence in order to gain insight into defence pathways against parasitic plants.

Finally, one significant outcome was the identification of 15 TCs without homologies to previously identified sequences. In addition to comprehensive collections, several plant genomes sequenced completely or sequenced to a large extent are available to date. The genome sequence of M. truncatula is expected throughout 2007 (http://www.medicago.org/genome). Thus, it might be anticipated that M. truncatula ESTs will match sequences from other plant EST or genome sequence data. The fact that no putative homologues have been identified in other plant genomes indicates that these genes could be extremely interesting for further functional studies and could reveal novel activated defence pathways. These gene products might not be involved in common defence responses and play a rather specific role during pathogenic legume–Orobanche interactions.

5 Concluding remarks

This is the first application of SSH to study the molecular changes of the model legume M. truncatula in response to Orobanche. A significant number of entries of this collection have shown homology with previously described genes already known to be involved in different plant responses pathways and resistance mechanisms activated during several plant–pathogen interactions. Although several cDNAs fragments were aligned with described sequences, the function of most of them is still unknown. Moreover, 18% of the Orobanche-induced ESTs seems to be new sequences since they have not matched entries of large scale M. truncatula or other organisms sequencing projects. Thus, the SSH approach and EST sequencing has proven also to be a powerful tool for identifying novel M. truncatula genes specifically regulated in the interaction with O. crenata. Although additional studies are necessary, the induced genes identified here represent a comprehensive resource for functional characterizations in the T-DNA or TILLING mutant collections currently established for different legume species that are affected by O. crenata. These studies will contribute to elucidate the molecular basis of resistance to this parasitic plant in legumes. Moreover, considering the sinteny relations between M. truncatula and economically important grain legume crops severely affected by O. crenata, our results could have direct implications in future crop breeding programmes.

Acknowledgements

Jose Die was a visiting researcher at the Department of Molecular Genetics at the University Hannover (Germany) funded by the STSM-COST-849 Action and GLIP. We are grateful to Burkhard Linke (Bioinformatics Resource Facility, CeBiTec, Bielefeld University) for the RT-PCR primers design, and to FP6-2002-FOOD-1-506223 project for financial support.

References

[1] Joel DM, Hershenhorn Y, Eizenberg H, Aly R, Ejeta G, Rich PJ, et al. Biology and management of weedy root parasites. In: Janick J, editor. Horticutural reviews. New York: Wiley; 2007. p. 267–350.
[2] Rubiales D, Pe´rez-de-Luque A, Ferna´ndez-Aparicio M, Sillero JC, Roma´n B, Kharrat M, et al. Screening techniques and sources of resistance against parasitic weeds in grain legumes. Euphytica 2006; 147:187–99.
[3] Cubero JI, Herna´ndez L. Breeding faba bean (Vicia faba L.) for resistance to Orobanche crenata Forsk. Options Me´diterr 1991;10: 51–7.
[4] Westwood JH. Characterization of the Orobanche–Arabidopsis system for studying parasite–host interactions. Weed Sci 2000;48: 742–8.
[5] Joel DM, Portnoy VH. The angiospermous root parasite Orobanche L. (Orobanchaceae) induces expression of a pathogenesis related (PR) gene in susceptible tobacco roots. Ann Bot 1998;81:779–81.
[6] Westwood JH, Yu X, Foy CL, Cramer CL. Expression of a defenserelated 3-hydroxy-3-methylglutaryl CoA reductase gene in response to parasitization by Orobanche spp. Mol Plant Microbe Interact 1998;11:530–6.
[7] Dos Santos CV, Letousey P, Delavault P, Thalouarn P. Defense gene expression analysis of Arabidopsis thaliana parasitized by Orobanche ramosa. Phytopathology 2003;93:451–7.
[8] Dos Santos CV, Delavault P, Letousey P, Thalouarn P. Identification by suppression subtractive hybridization and expression analysis of Arabidopsis thaliana putative defence genes during Orobanche ramosa infection. Physiol Mol Plant Pathol 2003;62:297–303.
[9] Dita MA, Rispail N, Prats E, Rubiales D, Singh KB. Biotechnology approaches to overcome biotic and abiotic stress constraints in legumes. Euphytica 2006;147:1–24.
[10] Rodrı´guez-Conde MF, Moreno MT, Cubero JI, Rubiales D. Characterization of the Orobanche-Medicago truncatula association for studying early stages of the parasite–host interaction. Weed Res 2004;44:218–23.
[11] VanderBosch K, Stacey G. Advances in legume biology. Plant Physiol 2003;131:839.
[12] Hohnjec N, Vieweg MF, Puhler A, Becker A, Ku¨ster H. Overlaps in the transcriptional profiles of Medicago truncatula roots inoculated with two different glomus fungi provide insights into the genetic program activated during arbuscular mycorrhiza. Plant Physiol 2005;137:1283–301.
[13] Ku¨ster H, Hohnjec N, Krajinski F, El Yahyaoui F, Manthey K, Gouzy J, et al. Construction and validation of cDNA-based Mt6kRIT macro- and microarrays to explore root endosymbioses in the model legume Medicago truncatula. J Biotechnol 2004;108:95–113.
[14] Gonzalez-Verdejo CI, Barandiaran X, Moreno MT, Cubero JI, Di Pietro A. An improved axenic system for studying pre-infection development of the parasitic plant Orobanche ramosa. Ann Bot 2005;96:1121–7.
[15] van Hezewijk MJ, van Beem AP, Verkleij JAC, Pieterse AH. Germination of Orobanche crenata seeds, as influenced by conditioning temperature and period. Can J Bot 1993;71:786–92.
[16] Pe´rez-De-Luque A, Rubiales D, Cubero JI, Press MC, Scholes J, Yoneyama K, et al. Interaction between Orobanche crenata and its host legumes: unsuccessful haustorial penetration and necrosis of the developing parasite. Ann Bot 2005;95:935–42.
[17] Diatchenko L, Lau YFC, Campbell AP, Chenchik A, Moqadam F, Huang B, et al. Suppression subtractive hybridization: a method for generating differentially regulated or tissue-specific cDNA probes and libraries. Proc Natl Acad Sci USA 1996;93:6025–30.
[18] Ewing B, Hillier L, Wendl M, Green P. Base-calling of automated sequencer traces using phred I. Accuracy assessment. Genome Res 1998;8:175–85.
[19] Ewin B, Green P. Base-calling of automated sequencer traces using phred II. Error probabilities. Genome Res 1998;8:186–94.
[20] Liang F, Holt I, Pertea G, Karamycheva S, Salzberg SL, Quackenbush J. An optimized protocol for analysis of EST sequences. Nucleic Acids Res 2000;28:3657–65.
[21] Huang X, Madan A. CAP3: a DNA sequence assembly program. Genome Res 1999;9:868–77.
[22] Altschul SF, Madden TL, Schaffer AA, Zhang JH, Zhang Z, Miller W, et al. Gapped BLAST and PSI-BLAST: a new generation of protein database search programs. Nucleic Acids Res 1997;25: 3389–402.
[23] Hohnjec N, Perlick AM, Puhler A, Ku¨ster H. The Medicago truncatula sucrose synthase gene MtSucS1 is activated both in the infected region of root nodules and in the cortex of roots colonized by arbuscular mycorrhizal fungi. Mol Plant Microbe Interact 2003;16: 903–15.
[24] Journet EP, van Tuinen D, Gouzy J, Crespeau H, Carreau V, Farmer MJ, et al. Exploring root symbiotic programs in the model legume Medicago truncatula using EST analysis. Nucleic Acids Res 2002;30: 5579–92.
[25] Ivashuta S, Uchiyama K, Gau M, Shimamoto Y. Linear amplification coupled with controlled extension as a means of probe amplification in a cDNA array and gene expression analysis during cold acclimation in alfalfa (Medicago sativa L.). J Exp Bot 2002; 367:351–9. [26] Joel DM. The long-term approach to parasitic weeds control: manipulation of specific developmental mechanisms of the parasite. Crop Prot 2000;19:753–8.
[27] Sillero JC, Moreno MT, Rubiales D. Sources of resistance to crenate broomrape in Vicia species. Plant Dis 2005;89:22–7.
[28] Rubiales D, Pe´rez-de-Luque A, Joel DM, Alca´ntara C, Sillero JC. Characterization of resistance in chickpea to crenate broomrape (Orobanche crenata). Weed Sci 2003;51:702–7.
[29] Serghini K, Pe´rez-de-Luque A, Castejo´n-Mun˜oz M, Garcı´a-Torres L, Jorrı´n JV. Sunflower (Helianthus annuus L.) response to broomrape (Orobanche cernua Loefl.) parasitism: induced synthesis and excretion of 7-hydroxylated simple coumarins. J Exp Bot 2001;52: 2227–34.
[30] Pe´rez-de-Luque A, Jorrı´n J, Cubero JI, Rubiales D. Orobanche crenata resistance and avoidance in pea (Pisum spp.) operate at different developmental stages of the parasite. Weed Res 2005;45: 379–87.
[31] Pe´rez-de-Luque A, Gonza´lez-Verdejo CI, Lozano MD, Dita MA, Cubero JI, Gonza´lez-Melendi P, et al. Protein cross-linking, peroxidase and b1,3-endoglucanase involved in resistance of pea against Orobanche crenata. J Exp Bot 2006;57:1461–9.

[32] Pe´rez-de-Luque A, Lozano MD, Cubero JI, Gonza´lez-Melendi P, Risuen˜o MC, Rubiales D. Mucilage production during the incompatible interaction between Orobanche crenata and Vicia sativa. J Exp Bot 2006;57:931–42.
[33] Rubiales D, Alca´ntara C, Pe´rez-de-Luque A, Gil J, Sillero JC. Infection of chickpea (Cicer arietinum) by crenate broomrape (Orobanche crenata) as influenced by sowing date and weather conditions. Agronomie 2003;23:359–62.
[34] Castillejo MA, Maldonado AM, Dumas-Gaudot E, Ferna´ndezAparicio M, Susin R, Rubiales D, et al. Differential expression proteomics to investigate responses and resistance to Orobanche crenata in Medicago truncatula. Plant Physiol 2007, in press.
[35] Liu JY, Blaylock LA, Endre G, Cho J, Town CD, VandenBosch KA, et al. Transcript profiling coupled with spatial expression analyses reveals genes involved in distinct developmental stages of an arbuscular mycorrhizal symbiosis. Plant Cell 2003;15:2106–23.
[36] Wulf A, Manthey K, Doll J, Perlick AM, Linke B, Bekel T, et al. Transcriptional changes in response to arbuscular mycorrhiza development in the model plant Medicago truncatula. Mol Plant Microbe Interact 2003;16:306–14.
[37] Grunwald U, Nyamsuren O, Tamasloukht M, Lapopin L, Becker A, Mann P, et al. Identification of mycorrhiza-regulated genes with arbuscule development-related expression profile. Plant Mol Biol 2004;55:553–66.
[38] Torregrosa CA, Dumas B, Krajinski F, Tugaye MT, Jacquet C. Transcriptomic approaches to unravel plant pathogen interactions in legumes. Euphytica 2006;147:25–36.
[39] Desai S, Hill J, Trelogan S, Diatchenko L, Siebert PD. Identification of differentially expressed genes by suppression substractive hybridization. In: Hunt S, Livesey F, editors. Functional genomics. Oxford: Oxford University Press; 2000. p. 81–112.
[40] Dixon RA, Achnine L, Kota P, Liu CJ, Reddy MSS, Wang LJ. The phenylpropanoid pathway and plant defence—a genomics perspective. Mol Plant Pathol 2002;3:371–90.
[41] Dixon RA, Harrison MJ, Paiva NL. The isoflavonoid phytoalexin pathway—enzymes to genes to transcription factors. Physiol Plant 1995;93:385–92.
[42] Glazebrook J. Contrasting mechanisms of defense against biotrophic and neotrophic pathogens. Ann Rev Phytopathol 2005;43:205–27.
[43] Thomma B, Nelissen I, Eggermont K, Broekaert WF. Deficiency in phytoalexin production causes enhanced susceptibility of Arabidopsis thaliana to the fungus Alternaria brassicicola. Plant J 1999;19:163–71.
[44] Ichinose Y, Hisiyasu Y, Sanematsu S, Ishiga Y, Seki H, Toyoda K, et al. Molecular cloning and functional analysis of pea cDNA E86 encoding homologous protein to hypersensitivity-related hsr203J. Plant Sci 2001;160:997–1006.
[45] Pontier D, Godiard L, Marco Y, Roby D. hsr203J, a tobacco gene whose activation is rapid, highly localized and specific for incompatible plant/pathogen interactions. Plant J 1994;5:507–21.
[46] Baudouin E, Charpenteau M, Roby D, Marco Y, Ranjeva R, Ranty B. Functional expression of a tobacco gene related to the serine hydrolase family. Esterase activity towards short chain dinitrophenyl acylesters. Eur J Biochem 1997;248:700–6.
[47] Lane JA, Moore THM, Child DV, Cardwell KE, Singh BB, Bailey JA. Virulence characteristics of a new race of the parasitic angiosperm Striga gesneroides from southern Benin on cowpea. Euphytica 1994;72:183–8.
[48] Lozano MD, Moreno MT, Rubiales D, Pe´rez-de-Luque A. Medicago truncatula as a model host for legumes-parasitic plants interactions: two phenotypes of resistance for one defensive mechanism. Plant Physiol 2007, in press.
[49] Lacombe E, Hawkins S, Van Doorsselaere J, Piquemal J, Goffner D, Poeydomenge O, et al. Cinnamoyl CoA reductase, the first committed enzyme of the lignin branch biosynthetic pathway: cloning, expression and phylogenetic relationships. Plant J 1997;11:429–41.
[50] Goujon T, Ferret V, Mila I, Pollet B, Ruel K, Burlat V, et al. Downregulation of the AtCCR1 gene in Arabidopsis thaliana: effects on phenotype, lignins and cell wall degradability. Planta 2003;217: 218–28.
[51] Piquemal J, Lapierre C, Myton K, O'Connell A, Schuch W, GrimaPettenati J, et al. Down-regulation of cinnamoyl-CoA reductase induces significant changes of lignin profiles in transgenic tobacco plants. Plant J 1998;13:71–83.
[52] Lauvergeat V, Lacomme C, Lacombe E, Lasserre E, Roby D, GrimaPettenati J. Two cinnamoyl-CoA reductase (CCR) genes from Arabidopsis thaliana are differentially expressed during development and in response to infection with pathogenic bacteria. Phytochemistry 2001;57:1187–95.
[53] Mulder NJ, Apweiler R, Attwood TK, Bairoch A, Bateman A, Binns D, et al. InterPro, progress and status in 2005. Nucleic Acids Res 2005;33:201–5.
[54] Moiseyev GP, Fedoreyeva LI, Zhuravlev YN, Yasnetskaya E, Jekel Pa, Beintema JJ. Primary structures of two ribonucleases from ginseng calluses—new members of the PR-10 family of intracellular pathogenesis-related plant proteins. FEBS Lett 1997;407: 207–10.
[55] Park CJ, Kim KJ, Shin R, Park JM, Shin YC, Paek KH. Pathogenesis-related protein 10 from hot pepper functions as a ribonuclease in an antiviral pathway. Plant J 2004;37:186–98. [56] Press MC, Gravest JD, Stewart GR. Physiology of the interaction of angiosperm parasites and their higher plant hosts. Plant Cell Environ 1990;13:91–104.
[57] Hibberd JM, Quick P, Press MC, Scholes JD, Jeschke WD. Solute fluxes from tobacco to the parasitic angiosperm Orobanche cernua and the influence on infection on host carbon and nitrogen relations. Plant Cell Environ 1999;22:937–47.

Figures

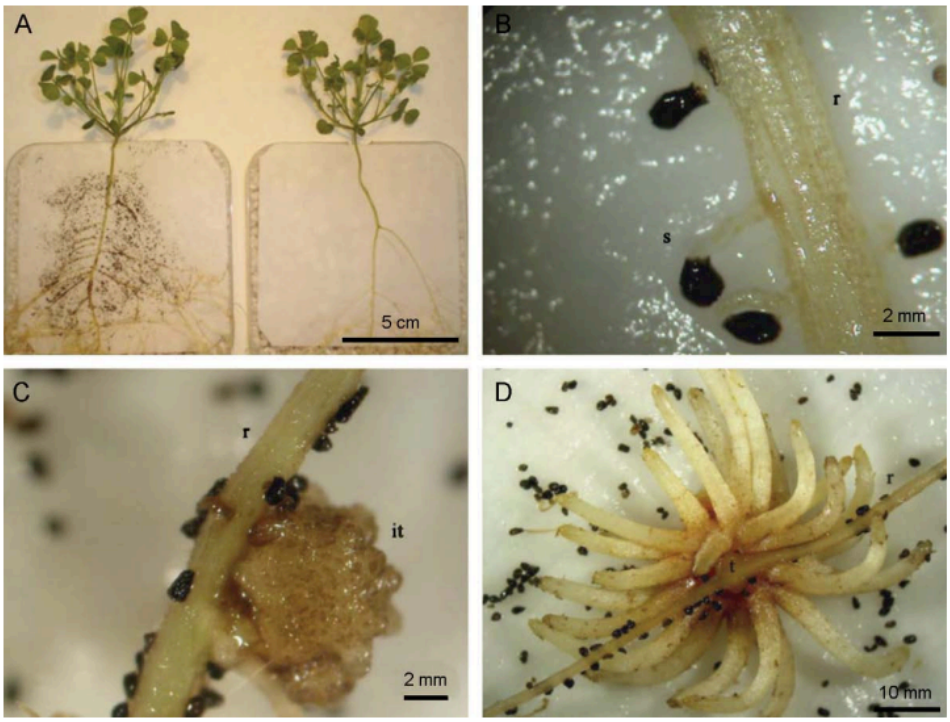

Fig. 1 Stages of parasitization process of Orobanche crenata in Medicago truncatula (SA4087). (A) Infected and control plants in the dish system. (B) Germinated seeds (s) of O. crenata at early stages of parasitization on M. truncatula roots (r), 15 days post inoculation (dpi). (C) Initial stages of tubercle (it) formation of O. crenata in SA4087 roots (r), 21 dpi. (D) Well-developed tubercles (t) of O. crenata in M. truncatula roots (r), 35 dpi.

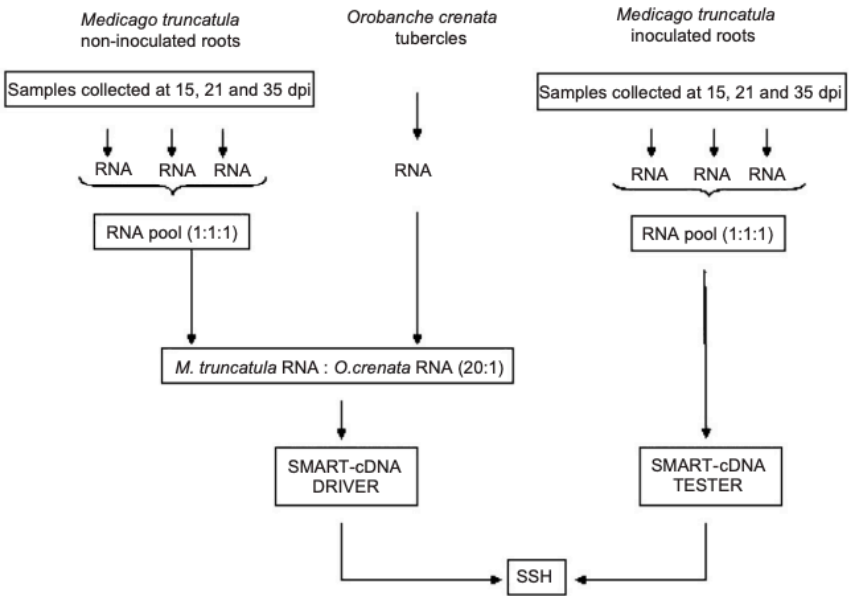

Fig. 2 Flowchart of the experimental design to obtain a cDNA-library enriched for genes specifically induced in M. truncatula in response to O. crenata parasitization.

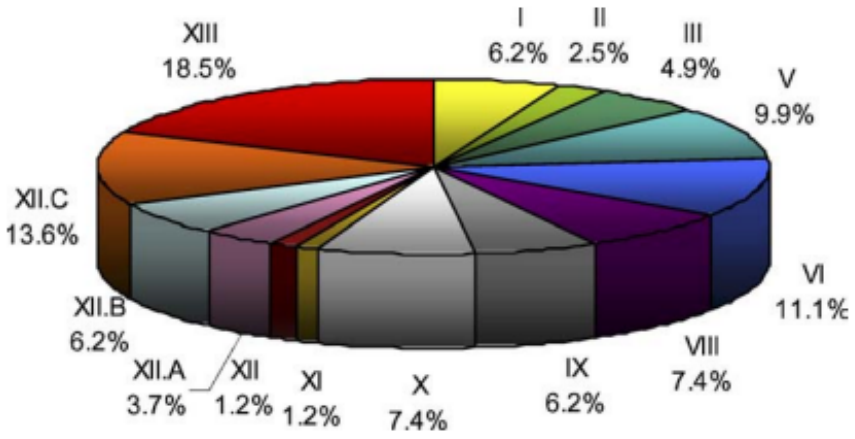

Fig. 3 A pie chart showing the fraction on differentially genes in functional categories according to Journet et al. [24] as follows: (I) cell wall; (II) cytoskeleton; (III) membrane transport; (V) primary metabolism; (VI) secondary metabolism and hormone metabolism; (VIII) gene expression and rna metabolism; (IX) protein synthesis and processing; (X) signal transduction and post-translational regulation; (XI) cell division cycle; (XII.A) defence and cell rescue; (XII.B) abiotic stimuli and development; (XII.C) unknown function; (XIII) no homology.

Tables

Table 1. Primer sequences used for quantitative real-time reverse transcription polymerase chain reaction

Annotation	MtGI-TC[a]	Left primer (5′–3′)	Right primer (5′–3′)
Acid phosphatase	TC93960	atgtcatggtaatgttcaaaa	ggcataataaggaaggttaga
Receptor-like protein kinase	TC94311	ttgtgtttgttttagcgtatt	gagtgaatttccttcctaaaa
Caffeoyl-CoA O-methyltransferase	TC94321	acctctcgttcaagattacat	ttatatccatccaacaactca
Glutathione S-transferase	TC95046	gtacctcaaattacagccttt	ttgcttcactttcttcaatta
Dehydrin-like protein	TC100921	tcaatatcaacaaggttatgg	ggtacttccatattcagtggt
Ripening-related protein	TC106505	ggggaaaatgtagctctataa	attcatttatttgcatcacac
Chalcone synthase 2	TC106537	gaacacaaaactgaactcaaa	caagagtttggtgagttgata
Chalcone synthase	TC106550	gggaatttctgattacaactc	actgtttcaatggtaagtcct
Aluminium-induced protein	TC106693	ctacgagaacttctgaaacct	aaaatttttgttctccttctg
P450 monooxygenase	TC106704	tcaaagattgacacttctgag	aaaaatcatctcaaaaccatt
Cinnamoyl-CoA reductase	TC106830	gtgttgatgtagaggttgatg	gtatgtgagctaatgcaacat
hsr203J homolog	TC107779	ttggcttagaatttacaatga	ctcggtgtagacatggtagta
P450 hydroxylase	TC107779	ttggcttagaatttacaatga	ctcggtgtagacatggtagta
Expansin-like protein	TC108173	ctcttctataatggagctggt	cctactatctctgtttgaccc
Small heat schock protein	TC108710	gtagatcttcctggtttgaag	tcactcttcttctcttctcc
Unknown protein	TC110611	ttactgatgtcacagagcttc	gaggaatttgattttgctagt

[a]MtGI, *Medicago truncatula* Gene Index; TC, tentative consensus sequence.

Table 2. Summary of sequence analysis of supresion subtractive hybridization library.

	Clones	Clusters
Secuenced cDNAs	288	–
ESTs identified	267	81
Known function	175	55
Unknown function	60	11
No EST match	32	15

Table 3. Annotation of ESTs obtained by SSH during M. truncatula–O. crenata interaction

TIGR ID[a]	Annotation[b]	Length (bp)	e-Value	N[c]
I. Cell wall				
TC108173	Expansin-like protein	558	$1.4e^{-89}$	8
TC94321	Caffeoyl-CoA O-methyltransferase	699	$1.3e^{-127}$	3
TC94419	Early nodulin 12A precursor (N-12A)	576	$2.0e^{-45}$	1
TC106830	Cinnamoyl-CoA reductase	392	$1.4e^{-65}$	1
II. Cytoskeleton				
TC107712	Myosin II heavy chain-like	371	$1.5e^{-58}$	4
TC257340	Kinesin-like protein	744	$5.0e^{-37}$	2
III. Membrane transport				
TC110186	Putative magnesium transporter	875	$3.3e^{-50}$	2
TC101253	Calcium ion binding	809	$1.0e^{-138}$	2
TC100732	Eukaryotic porin	611	$4.8e^{-65}$	1
TC106921	Membrane transporter	382	$1.1e^{-56}$	1
V. Primary metabolism				
TC94198	NADH dehydrogenase-related	478	$5.9e^{-49}$	22
TC93941	Delta 1-pyrroline-5-carboxylate synthetase	485	$8.0e^{-38}$	19
TC112168	Glutaredoxin-like protein	521	$1.6e^{-82}$	3
TC93960	Acid phosphatase	478	$1.4e^{-73}$	2
TC95361	Adenosine monophosphate binding protein	499	$1.4e^{-79}$	1
TC100662	Alcohol dehydrogenase 1	522	$1.8e^{-88}$	1
TC99978	NADH dehydrogenase subunit 2	531	$5.5e^{-66}$	1
TC106975	Alpha-L-arabinofuranosidase	509	$1.2e^{-91}$	1

Table 3. (Cont.)

TIGR ID[a]	Annotation[b]	Length (bp)	e-Value	N[c]
VI. Secondary and hormone metabolism				
TC106704	Cytochrome P450: *trans*-cinnamate 4-monooxygenase	396	$3.3e^{-64}$	26
TC100569	Farnesyl pyrophosphate synthetase 1	816	$1.7e^{-145}$	6
TC106537	Chalcone synthase 2	790	$6.0e^{-127}$	3
TC107984	Cytochrome P450-dependent fatty acid hydroxylase	686	$2.2e^{-73}$	2
TC95046	Glutathione S-transferase GST 24	586	$6.2e^{-101}$	1
TC106550	Chalcone synthase	503	$5.3e^{-48}$	1
TC107322	Allene oxide cyclase precursor	688	$2.8e^{-107}$	1
TC108709	1-aminocyclopropane-1-carboxylate oxidase	598	$1.2e^{-90}$	1
TC109903	Benzoyltransferase-like protein	521	$4.2e^{-29}$	1
VIII. Gene expression and RNA metabolism				
TC94391	Small nuclear ribonucleoprotein-like protein	495	$4.1e^{-78}$	2
TC101721	Small nuclear ribonucleoprotein	651	$6.9e^{-101}$	2
TC106884	Protein disulfide-isomerase A6 precursor	842	$1.4e^{-139}$	2
TC108710	Small heat shock protein	572	$1.2e^{-17}$	2
TC94400	RNA binding protein homolog	742	$6.1e^{-132}$	1
TC97792	U1 small nuclear ribonucleoprotein	597	$2.5e^{-30}$	1
IX. Protein synthesis and processing				
TC100531	60S ribosomal protein L6	542	$5.1e^{-88}$	7
TC100590	40S ribosomal protein S16	201	$5.1e^{-28}$	2
AJ621860	60S ribosomal protein L18a	796	$3.9e^{-14}$	2
TC106383	Ribosomal protein L2	342	$4.6e^{-53}$	1
TC108361	Putative 50S ribosomal protein L27	470	$1.3e^{-32}$	1
X. Signal transduction and post-translational regulation				
TC107122	Leucine-rich repeat family protein/protein kinase family	641	$1.0e^{-110}$	11
TC106520	Ubiquitin carboxyl-terminal hydrolase	364	$3.6e^{-33}$	3
TC94311	Receptor-like protein kinase	544	$1.6e^{-85}$	2
TC93955	GTP-binding protein	520	$9.2e^{-86}$	1
TC93994	GTP-binding protein	497	$1.2e^{-78}$	1
TC94058	GTP-binding protein	233	$3.7e^{-37}$	1
XI. Cell division cycle				
TC100539	Guanine nucleotide-binding beta subunit protein	529	$6.8e^{-25}$	2
XII. Miscellaneous				
TC101253	Calcium ion binding	809	$1.0e^{-138}$	2
TC102537	TATA box binding protein associated factor-like protein	658	$3.5e^{-90}$	1
XII.A. Defense and cell rescue				
TC101330	Defense-related protein	454	$3.5e^{-38}$	2
TC107779	Hypersensitive reaction 203J homolog	502	$2,1e^{-192}$	1
TC109758	Hypersensitive reaction 203J homolog	558	$8.2e^{-84}$	1
XII.B Abiotic stimuli and development				
TC106505	Ripening-related protein	553	$3.6e^{-88}$	2
TC106693	Aluminium-induced protein	815	$2.6e^{-132}$	2
TC107018	SIEP1L protein precursor	541	$3.2e^{-87}$	2
TC100921	Dehydrin-like protein	564	$8.7e^{-63}$	1
TC106492	Ripening related protein	502	$2.5e^{-77}$	1
XII.C Unknown function				
TC106844	Hypothetical protein	529	$3.0e^{-76}$	28
TC97187	KED protein	622	$4.3e^{-24}$	14
TC110611	Unknown protein	586	$3.0e^{-21}$	10
TC94076	Unknown protein	727	$4.3e^{-118}$	1
TC94208	Unknown protein	638	$5.0e^{-29}$	1
TC108983	Unknown protein	598	$6.1e^{-67}$	1
TC109362	Unknown protein	422	$4.1e^{-64}$	1
TC109584	Unknown protein	617	$5.8e^{-38}$	1
TC110220	Unknown protein	732	$5.1e^{-88}$	1
TC111136	Unknown protein	651	$4.0e^{-54}$	1

[a]Identifier in the TIGR *M. truncatula* Gene Index grouped into functional categories according to Journet et al. [24].
[b]Updated annotations according to the current TIGR *M. truncatula* Gene Index (TIGR/MtGI 8.0) and UniProt, Interpro searches.
[c]*N*, Number of cDNA clones in the library.

Table 4. Verification of Orobanche crenata induced M. truncatula genes represented by tentative consensus sequences (TCs) by quantitative real-time RT-PCR (qRT-PCR)

TIGR ID	Annotation	Induction
I. Cell wall		
TC94321	Caffeoyl-CoA O-methyltransferase	8.93
TC106830	Cinnamoyl-CoA reductase	**5.62**
TC108173	Expansin-like protein	**1.46**
V. Primary metabolism		
TC93960	Acid phosphatase	**2.83**
VI. Secondary and hormone metabolism		
TC95046	Glutathione S-transferase GST 24	2.99
TC106550	Chalcone synthase	**1.41**
TC106537	Chalcone synthase 2	**1.54**
TC106704	Cytochrome P450: Trans-cinnamate 4-monooxygenase	**1.87**
TC107984	Cytochrome P450-dependent fatty acid hydroxylase	8.38
VIII. Gene expression and RNA metabolism		
TC108710	Small heat shock protein	**9.91**
X. Signal transduction and post-translational regulation		
TC94311	Receptor-like protein kinase	**3.84**
XII.A. Defense and cell rescue		
TC107779	Hypersensitive reaction 203J homolog	**3.25**
XII.B Abiotic stimuli and development		
TC100921	Dehydrin-like protein	**244.05**
TC106505	Ripening-related protein	**2.39**
TC106693	Aluminium-induced protein	**1.91**
XII.C Unknown function		
TC110611	Unknown protein	**3.09**

Values shown indicate average relative expression ratio to control (data from three independent experiments with three biological replicates). Bold text indicates statistically significant induction ($P \leqslant 0.05$).